

## Unified picture of modal loss rates from microwave to optical frequencies in deep-subwavelength metallic structures: A case study with slot waveguides

Wonseok Shin and Shanhui Fan

Citation: [Applied Physics Letters](#) **107**, 171102 (2015); doi: 10.1063/1.4934707

View online: <http://dx.doi.org/10.1063/1.4934707>

View Table of Contents: <http://scitation.aip.org/content/aip/journal/apl/107/17?ver=pdfcov>

Published by the [AIP Publishing](#)

---

### Articles you may be interested in

[High efficiency coupling of radio frequency beams from the dual frequency gyrotron with a corrugated waveguide transmission system](#)

*Rev. Sci. Instrum.* **84**, 013501 (2013); 10.1063/1.4772572

[Dual cylindrical metallic grating-cladding polymer hollow waveguide for terahertz transmission with low loss](#)

*Appl. Phys. Lett.* **97**, 133502 (2010); 10.1063/1.3491291

[Magnetic metal cladding gives better attenuation in small waveguides operating at high microwave frequencies than nonmagnetic metals](#)

*Appl. Phys. Lett.* **96**, 252506 (2010); 10.1063/1.3457478

[Projecting deep-subwavelength patterns from diffraction-limited masks using metal-dielectric multilayers](#)

*Appl. Phys. Lett.* **93**, 111116 (2008); 10.1063/1.2985898

[Metallic slit waveguide for dispersion-free low-loss terahertz signal transmission](#)

*Appl. Phys. Lett.* **90**, 061111 (2007); 10.1063/1.2472544

---

The logo for AIP APL Photonics is displayed on a red background with a bright yellow sunburst effect. The letters 'AIP' are in a large, white, sans-serif font, followed by a vertical bar and the words 'APL Photonics' in a smaller, white, sans-serif font.

AIP | APL Photonics

*APL Photonics* is pleased to announce  
**Benjamin Eggleton** as its Editor-in-Chief



# Unified picture of modal loss rates from microwave to optical frequencies in deep-subwavelength metallic structures: A case study with slot waveguides

Wonseok Shin<sup>a)</sup> and Shanhui Fan<sup>b)</sup>

*E. L. Ginzton Laboratory, Stanford University, Stanford, California 94305, USA*

(Received 7 July 2015; accepted 11 October 2015; published online 26 October 2015)

The behavior of the modal loss rate in deep-subwavelength metallic structures depends strongly on frequency: as the mode size decreases, at optical frequencies, the modal loss rate always increases to the theoretical upper bound  $\Gamma/2$ , whereas at microwave frequencies, it remains far lower than  $\Gamma/2$ , where  $\Gamma$  is the electron collision frequency of the metal. By analyzing the metallic slot waveguide as a model system, we show that these significantly different behaviors of the modal loss rate at optical and microwave frequencies are actually two extreme cases of a single universal behavior. Specifically, we show that as the mode size decreases, the loss rate always plateaus first and then increases to  $\Gamma/2$ , regardless of frequency. The only difference between frequencies is the properties of the plateau: at optical frequencies, the plateau is narrow, allowing the loss rate to reach  $\Gamma/2$  at a relatively large mode size, whereas at microwave frequencies, the plateau is wide and formed at  $\frac{1}{\sqrt{3}}\omega$ , defining a practically attainable maximum loss rate that is far lower than  $\Gamma/2$ . © 2015 AIP Publishing LLC. [<http://dx.doi.org/10.1063/1.4934707>]

Metallic structures provide the capability of manipulating electromagnetic (EM) fields at deep-subwavelength scale. At radio and microwave frequencies, many components such as antennas and transmission lines rely on such a capability to collect and guide EM waves efficiently in a deep-subwavelength volume and area.<sup>1,2</sup> Similarly, at optical frequencies, there have been tremendous efforts toward manipulating EM waves at deep-subwavelength scale by utilizing metallic structures, as evidenced by the recent progress in plasmonics and optical metamaterials.<sup>3,4</sup>

Because metals are always lossy, understanding the behavior of the loss rate of the deep-subwavelength EM modes supported by metallic structures is of fundamental technological importance. For all frequencies  $\omega$  ranging from radio to visible frequencies, the permittivity of a free-electron metal is described by the Drude model as

$$\epsilon_m(\omega) = \epsilon_\infty \left( 1 - \frac{\omega_p^2}{\omega(\omega - i\Gamma)} \right), \quad (1)$$

where  $\epsilon_\infty$  is the value of  $\epsilon_m$  at  $\omega = \infty$ ,  $\omega_p$  is the plasma frequency of the metal, and  $\Gamma$  is the electron collision frequency of the metal.

It has been shown that for any structures consisting of such a metal and lossless dielectrics, the loss rates of the EM modes are always bounded above by  $\Gamma/2$ .<sup>5-8</sup> Furthermore, at optical frequencies, it has been shown that the modal loss rates do approach this upper bound for modes whose dimension is a fraction of the free-space wavelength<sup>6-8</sup> (though for subnanometer structures this upper bound can be exceeded as the classical Drude model breaks down due to surface effects<sup>9</sup>).

On the other hand, at microwave frequencies, the modal loss rates are far below the upper bound in practice, even for deep-subwavelength modes.<sup>7</sup> For example, typical values of

$\Gamma/2$  of metals are in the order of  $10^{14} \text{ s}^{-1}$ .<sup>10</sup> A waveguide mode with such a loss rate would have a propagation distance of  $v_g/(\Gamma/2) \ll c/(\Gamma/2)$ , where  $v_g$  is the group velocity of the mode and  $c$  is the speed of light, and therefore would have a propagation distance in the order of micrometers or less. In reality, however, at a microwave frequency of 1 GHz, the standard coaxial cables, which have deep-subwavelength cross sections, have propagation distances in the order of several meters.<sup>1</sup> Thus, at microwave frequencies, the modal loss rates are in fact far below  $\Gamma/2$  in typical subwavelength structures.

In this letter, we take a step toward developing a theoretical picture that unifies such significantly different loss behaviors of deep-subwavelength modes at optical and microwave frequencies. For that purpose, we examine a metallic slot waveguide<sup>11</sup> illustrated in Fig. 1 as a model system. The waveguide is composed of a narrow dielectric slot of width  $d$  and permittivity  $\epsilon_d$ , embedded in an infinite metal of the permittivity  $\epsilon_m$  of Eq. (1).

The choice of the metallic slot waveguide as a model system has a number of merits: (a) it supports a tightly confined mode within the slot,<sup>12</sup> so it is straightforward to obtain a deep-subwavelength mode by simply narrowing the slot;

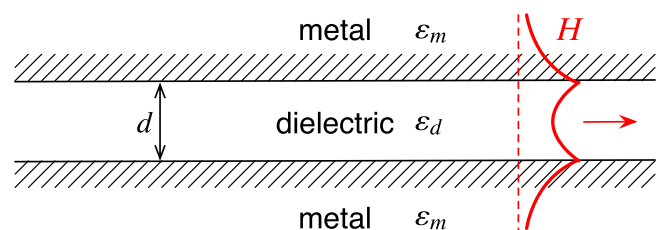


FIG. 1. Metallic slot waveguide and its fundamental mode. The waveguide is composed of a dielectric slot of width  $d$  embedded in an infinite metal. Its fundamental mode, whose out-of-page  $H$ -field has the magnitude illustrated by the red curve, propagates with wavenumber  $\beta$  and temporal loss rate  $\gamma$  at frequency  $\omega$ . The permittivities of the dielectric and metal are  $\epsilon_d$  and  $\epsilon_m$ , where  $\epsilon_m$  is described by the Drude model.

<sup>a)</sup>Electronic mail: wsshin@stanford.edu

<sup>b)</sup>Electronic mail: shanhui@stanford.edu

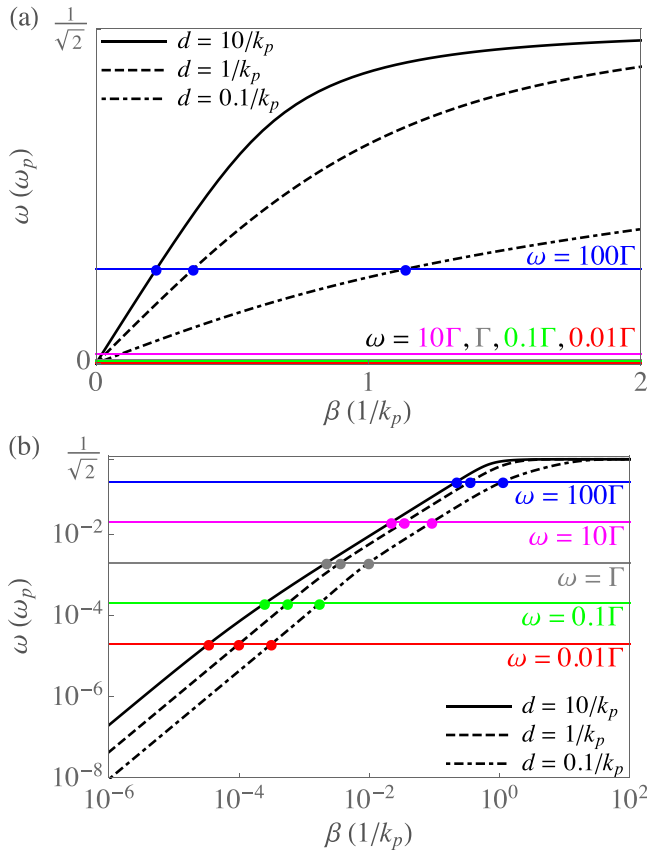


FIG. 2. (a)  $\omega$ - $\beta$  relation of the fundamental mode of the metallic slot waveguide for three slot widths  $d = 10/k_p, 1/k_p, 0.1/k_p$ , where  $k_p = \omega_p \sqrt{\mu_0 \epsilon_0}$ . (b) The same  $\omega$ - $\beta$  relation in logarithmic scale. The horizontal lines indicate five frequencies  $\omega = 100\Gamma, 10\Gamma, \Gamma, 0.1\Gamma$ , and  $0.01\Gamma$ . The material parameters used are  $\epsilon_d = \epsilon_0, \epsilon_\infty = \epsilon_0$ , and  $\Gamma = 0.002\omega_p$ .

(b) its simple structure allows us to analyze the modal loss rate analytically from the waveguide dispersion relation; (c) it is one of the most widely used waveguides in plasmonics,<sup>13–16</sup> so the thorough understanding of its modal loss behavior is of practical importance; (d) at deep-subwavelength scale, it often approximates waveguides with more complex geometry accurately,<sup>17</sup> so its understanding can be directly extended to a variety of waveguides; (e) its metal-dielectric-metal structure is often the basic building block of more complex systems such as hyperbolic metamaterials,<sup>18</sup> so its understanding can provide insights into systems beyond waveguides.

In our analysis, we solve for modes whose temporal and longitudinal dependences are in the form of  $e^{i(\Omega t - \beta z)}$ , where the propagation wavenumber  $\beta$  along the longitudinal direction  $z$  is taken to be real; the complex eigenfrequency  $\Omega = \omega + i\gamma$  has the oscillation frequency  $\omega$  and loss rate  $\gamma$  of the mode as the real and imaginary parts.<sup>19</sup> Note that the imaginary part of the complex frequency can be nonzero only in the presence of loss. This is in contrast to an alternative approach that uses real frequency and complex wavenumber, whose imaginary part can be nonzero even in the absence of loss.<sup>20,21</sup>

We consider the fundamental mode of the waveguide, whose dispersion relation is<sup>22</sup>

$$\tanh\left(\kappa_d \frac{d}{2}\right) = -\frac{\kappa_m / \kappa_d}{\epsilon_m / \epsilon_d}, \quad (2)$$

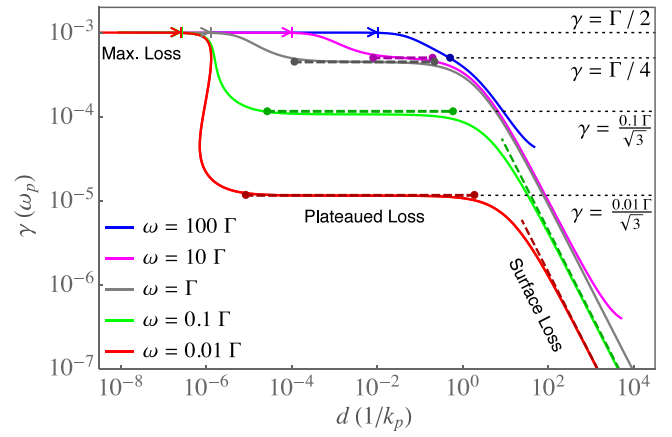


FIG. 3.  $\gamma$ - $d$  relation of the fundamental mode of the metallic slot waveguide for the five different frequencies  $\omega = 100\Gamma, 10\Gamma, \Gamma, 0.1\Gamma$ , and  $0.01\Gamma$  corresponding to the horizontal lines in Fig. 2. The dashed lines and arrowheads indicate the estimates from our theory. The material parameters used are  $\epsilon_d = \epsilon_0, \epsilon_\infty = \epsilon_0$ , and  $\Gamma = 0.002\omega_p$ . For  $\omega = 0.01\Gamma$ , the three values of  $\gamma$  at  $d \sim 10^{-6}/k_p$  are due to negative group velocity existing in the  $\omega$ - $\beta$  relation for such extremely small  $d$ .

where

$$\begin{aligned} \kappa_d &= \sqrt{\beta^2 - \Omega^2 \mu_0 \epsilon_d}, \\ \kappa_m &= \sqrt{\beta^2 - \Omega^2 \mu_0 \epsilon_m}. \end{aligned} \quad (3)$$

Here,  $\mu_0$  is the vacuum permeability, and the values of  $\epsilon_m$  at complex  $\Omega$ 's are obtained via analytic continuation of Eq. (1) into the complex plane. For numerical evaluation,  $\epsilon_d = \epsilon_0, \epsilon_\infty = \epsilon_0$ , and  $\Gamma = 0.002\omega_p$ , which correspond to air and silver,<sup>10</sup> are used throughout this letter.

From Eq. (2), we obtain the  $\omega$ - $\beta$  curve of the waveguide mode for a given  $d$ , as shown in Fig. 2. For every  $d$  considered in the figure, the waveguide supports a guided mode extending from  $\omega = 0$  to the surface plasmon frequency  $\omega_p / \sqrt{1 + \epsilon_d / \epsilon_\infty}$ . Note that  $\beta$  increases with decreasing  $d$  for a given  $\omega$ .

Now, we present the main result of our analysis: the  $\gamma$ - $d$  curve of the waveguide mode at different frequencies. Figure 3 shows the resulting  $\gamma$ - $d$  curve at five different frequencies  $\omega = 100\Gamma, 10\Gamma, \Gamma, 0.1\Gamma$ , and  $0.01\Gamma$ . As the slot width  $d$ , and thus the size of the waveguide mode, shrinks to deep-subwavelength scale, the modal loss rate  $\gamma$  exhibits a universal behavior regardless of  $\omega$ : it reaches a plateau first before eventually increasing to the theoretical upper bound  $\Gamma/2$ .

However, the strong dependence of the width and level of the plateau on  $\omega$  makes the behavior of the modal loss rate appear significantly different at optical and microwave frequencies. At optical frequencies ( $\omega \gg \Gamma$ ), a narrow plateau is formed at  $\gamma = \Gamma/4$  close to  $\Gamma/2$ , so  $\gamma$  increases quickly to  $\Gamma/2$  at a relatively large  $d$ , in a good agreement with the well-known behavior of the modal loss rate of plasmonic systems.<sup>5–8</sup> At microwave frequencies ( $\omega \ll \Gamma$ ), on the other hand, a wide plateau is formed at  $\gamma = \frac{1}{\sqrt{3}}\omega$ . Also, the wide plateau persists until the waveguide mode becomes unrealistically small: as shown in Fig. 3,  $\gamma$  approaches  $\Gamma/2$  only after  $d$  decreases approximately below  $10^{-6}/k_p = 10^{-6}\lambda_p/2\pi$ , which corresponds to an unrealistically narrow slot width of around  $10^{-4}$  nm for noble metals (e.g.,  $\lambda_p = 138$  nm for silver<sup>10</sup>). Therefore, at microwave

frequencies, reaching the theoretical upper bound  $\Gamma/2$  is rather hypothetical; instead, the plateau defines a practically attainable maximum loss rate at  $\frac{1}{\sqrt{3}}\omega$ , which is far lower than  $\Gamma/2$ .

Note also in Fig. 3 that for slot width less than or comparable to the plasma wavelength ( $d \lesssim 1/k_p$ ), the loss rate is an order of magnitude smaller at microwave frequencies than at optical frequencies, even though the degree of confinement compared to a wavelength is much stronger at microwave frequencies. This observation suggests that nanometer-scale structures, despite their small dimensions, may suffer from relatively low loss at microwave frequencies.

In the rest of the letter, we provide more detailed discussions on the behavior of  $\gamma$ . In Fig. 3, we consider three different regimes as  $d$  decreases: in the surface loss regime,  $\gamma$  increases; in the plateaued loss regime,  $\gamma$  plateaus; and in the maximum loss regime,  $\gamma$  reaches the theoretical upper bound  $\Gamma/2$ . Below, we derive the analytic expressions of  $\gamma$  in these three different regimes.

The frequency range considered in the derivation is  $\omega \ll \omega_p$ , which includes all frequencies from radio up to visible frequencies for the typical  $\omega_p$  of metals;<sup>10</sup> note that the five  $\omega$ 's chosen in Fig. 3 are within this range. Also, we assume  $\Gamma \ll \omega_p$ , as is typically the case for metals.<sup>10</sup> Then, Eq. (1) for complex frequency is approximated by

$$\varepsilon_m = -\varepsilon_\infty \frac{\omega_p^2}{\Omega(\Omega - i\Gamma)}, \quad (4)$$

because  $\gamma \leq \Gamma/2$  in  $\Omega = \omega + i\gamma$ , and thus the denominator in Eq. (4) is far less in magnitude than the numerator.

We begin with the maximum loss regime. We will show

$$\beta \gg |\Omega| \sqrt{\mu_0 |\varepsilon_m|}, \quad (5)$$

is the condition for  $\gamma$  to be in the maximum loss regime. Because  $|\varepsilon_m| \gg \varepsilon_d$  for  $\omega \ll \omega_p$ , Eq. (5) implies  $\beta \gg |\Omega| \sqrt{\mu_0 \varepsilon_d}$  as well. Hence, Eq. (3) is approximated by  $\kappa_d = \beta$  and  $\kappa_m = \beta$ , and Eq. (2) by

$$\tanh\left(\beta \frac{d}{2}\right) = -\frac{\varepsilon_d}{\varepsilon_m}. \quad (6)$$

Because the left-hand side and  $\varepsilon_d$  are real,  $\varepsilon_m$  should also be real for this equation to hold. From Eq. (4),  $\varepsilon_m$  is real if and only if  $\Omega(\Omega - i\Gamma) = (\omega + i\gamma)(\omega + i(\gamma - \Gamma))$  is real, or equivalently if  $2\gamma - \Gamma = 0$ . Therefore, when the condition (5) holds, we have

$$\gamma = \frac{\Gamma}{2}, \quad (7)$$

which is the modal loss rate in the maximum loss regime.

We can also obtain the condition on  $d$  for the maximum loss regime. Substituting Eq. (7) into Eq. (4), we get

$$\varepsilon_m = -\varepsilon_\infty \frac{\omega_p^2}{|\Omega|^2}. \quad (8)$$

Substituting Eq. (8) into Eq. (6) and using  $\tanh^{-1}\phi \simeq \phi$  for  $|\phi| \ll 1$ , we obtain an approximate expression of  $\beta$ . The expression is used in Eq. (5) to produce the condition

$$d \ll \frac{\varepsilon_d}{\varepsilon_\infty} \frac{2}{\omega_p \sqrt{\mu_0 \varepsilon_\infty}} \frac{\omega^2 + (\Gamma/2)^2}{\omega_p^2}, \quad (9)$$

for the maximum loss regime. Equation (9) indicates that the maximum loss regime begins at larger  $d$  for higher  $\omega$ . The range (9) of  $d$  is indicated by the arrowheads in Fig. 3. Note that for all  $\omega$ 's, the modal loss rate indeed reaches  $\Gamma/2$  in this range of  $d$ , though for  $\omega \ll \Gamma$  reaching such a loss rate requires unrealistically small  $d$  and therefore is hypothetical as mentioned earlier.

Next, we examine the plateaued loss regime. In this case, as compared with Eq. (5), we will show that

$$|\Omega| \sqrt{\mu_0 \varepsilon_d} \ll \beta \ll |\Omega| \sqrt{\mu_0 |\varepsilon_m|} \quad (10)$$

is the condition for  $\gamma$  to be in the plateaued loss regime. Under this condition, Eq. (3) is approximated by  $\kappa_d = \beta$  and  $\kappa_m = \Omega \sqrt{\mu_0 (-\varepsilon_m)}$ , and thus the dispersion relation (2) is approximated by

$$\tanh\left(\beta \frac{d}{2}\right) = -\frac{\Omega}{\beta} \sqrt{\mu_0 \frac{\varepsilon_d^2}{(-\varepsilon_m)}}. \quad (11)$$

Substituting Eq. (4) into Eq. (11), we obtain

$$\Omega^3(\Omega - i\Gamma) = \frac{4\omega_p^2 \varepsilon_\infty}{\mu_0 \varepsilon_d^2 d^2} \left[ \beta \frac{d}{2} \tanh\left(\beta \frac{d}{2}\right) \right]^2, \quad (12)$$

from which the relationship between the real and imaginary parts of  $\Omega$  can be inferred without explicitly calculating them. Suppose that  $\arg(\Omega) = \theta$ . Then, we have  $\tan \theta = \gamma/\omega$ . We also have  $\tan(-3\theta) = (\gamma - \Gamma)/\omega$ , because the right-hand side of Eq. (12) is positive and thus  $\arg(\Omega^3(\Omega - i\Gamma)) = 3\theta + \arg(\omega + i(\gamma - \Gamma)) = 0$ . Eliminating  $\gamma$  between the two trigonometric equations, we obtain

$$\tan \theta + \tan 3\theta = \Gamma/\omega, \quad (13)$$

whose solution  $\theta$  is used in the first trigonometric equation to describe the relationship between  $\omega$  and  $\gamma$  under the condition (10) as

$$\gamma = \omega \tan \theta. \quad (14)$$

Note that  $\theta$  dictated by Eq. (13) is independent of  $d$ . Therefore, Eq. (14) indicates the existence of the plateau under the condition (10) and provides an approximate value of the modal loss rate in the plateaued loss regime.

Equation (14) can be further approximated in the frequency regimes  $\omega \gg \Gamma$  and  $\omega \ll \Gamma$ . For  $\omega \gg \Gamma$ , we have  $\theta \ll 1$  from Eq. (13). Therefore, Eq. (13) is approximated by  $\theta + 3\theta = \Gamma/\omega$ , and Eq. (14) by

$$\gamma = \omega \theta = \frac{\Gamma}{4}, \quad (15)$$

for  $\omega \gg \Gamma$ . For  $\omega \ll \Gamma$ , on the other hand, the right-hand side of Eq. (13) increases toward infinity, so  $\tan 3\theta$  on the left-hand side, which increases faster than  $\tan \theta$ , should increase toward infinity as well. Therefore, we have  $\tan 3\theta \gg 1$ , or  $\theta \simeq \pi/6$ , and Eq. (14) is approximated by

$$\gamma = \frac{1}{\sqrt{3}}\omega, \quad (16)$$

for  $\omega \ll \Gamma$ . Hence, for  $\omega \ll \Gamma$ , the modal loss rate in the plateaued loss regime is independent of the dielectric and metal used in the slot waveguide.

We can also obtain the condition on  $d$  for the plateaued loss regime. Notice that the right-hand side of Eq. (12) is proportional to the form  $|\psi \tanh \psi|^2$ . Applying Eq. (10) on the right-hand side of the absolute value of Eq. (12) and using  $\psi_2 \tanh \psi_2 \gg \psi_1 \tanh \psi_1$  for  $\psi_2 \gg \psi_1 > 0$ , we can eliminate  $\beta$  from the inequalities. Subsequently, using  $\tanh^{-1} \phi \simeq \phi$  for  $|\phi| \ll 1$ , we obtain the condition

$$\frac{\varepsilon_d}{\varepsilon_\infty} \frac{2|1 - i(\Gamma/\Omega)|^{\frac{3}{2}} |\Omega|^2}{\omega_p \sqrt{\mu_0 \varepsilon_\infty} \omega_p^2} \ll d \ll \frac{2|1 - i(\Gamma/\Omega)|^{\frac{1}{2}}}{\omega_p \sqrt{\mu_0 \varepsilon_\infty}}, \quad (17)$$

for the plateaued loss regime, where  $\Omega = \omega + i\gamma$  has  $\gamma$  of Eq. (14). Equation (17) can be further simplified to

$$\frac{\varepsilon_d}{\varepsilon_\infty} \frac{2}{\omega_p \sqrt{\mu_0 \varepsilon_\infty}} \frac{\omega^2}{\omega_p^2} \ll d \ll \frac{2}{\omega_p \sqrt{\mu_0 \varepsilon_\infty}}, \quad (18)$$

for  $\omega \gg \Gamma$  using  $\gamma$  of Eq. (15), and

$$\frac{\varepsilon_d}{\varepsilon_\infty} \frac{2.15}{\omega_p \sqrt{\mu_0 \varepsilon_\infty}} \frac{\sqrt{\Gamma^3 \omega}}{\omega_p^2} \ll d \ll \frac{1.86}{\omega_p \sqrt{\mu_0 \varepsilon_\infty}} \sqrt{\frac{\Gamma}{\omega}}, \quad (19)$$

for  $\omega \ll \Gamma$  using  $\gamma$  of Eq. (16).

In Fig. 3, the horizontal dashed line segments are drawn at  $\gamma = \omega \tan \theta$  over the range (17) for  $\omega = \Gamma$ ; at  $\gamma = \Gamma/4$  over the range (18) for  $\omega = 100\Gamma, 10\Gamma$ ; at  $\gamma = \frac{1}{\sqrt{3}}\omega$  over the range (19) for  $\omega = 0.1\Gamma, 0.01\Gamma$ . The good agreement between the dashed line segments and the corresponding  $\gamma$ - $d$  curves validates our derivation. In the figure, for  $\omega \ll \Gamma$ , we observe a pronounced plateau that persists over a wide range of  $d$ . For  $\omega \gg \Gamma$ , on the other hand, the width of the plateau decreases quickly with increasing  $\omega$ : for  $\omega = 10\Gamma$ , we still observe a sizable plateau at  $\gamma = \Gamma/4$ , but for  $\omega = 100\Gamma$ , the plateau is no longer visible in the plot. Therefore, we see that the deep-subwavelength metallic slot waveguide mode has drastically different loss behaviors at optical and microwave frequencies.

Finally, we examine the surface loss regime. Here, we limit the analysis to microwave frequencies ( $\omega \ll \Gamma$ ), for which surface resistance can be defined.<sup>1</sup> (For optical frequencies, a similar result can be obtained using the field penetration depth into the metal.<sup>23</sup>) For the stored energy  $U$  and dissipating power  $P$ , the modal loss rate is expressed as  $\gamma = P/2U$ . By estimating  $P$  per unit area of the metal surface as  $\frac{1}{2}R_s|H_s|^2$  and  $U$  per unit volume within the slot as  $\frac{1}{2}\mu_0|H_s|^2$ , where  $H_s$  is the  $H$ -field on the metal surface,  $R_s = \sqrt{\mu_0\omega/2\sigma}$  is the surface resistance of the metal, and  $\sigma = \omega_p^2\varepsilon_\infty/\Gamma$  is the metal conductivity, we have

$$\gamma = \frac{1}{2} \frac{\int_0^{d/2} \frac{1}{2} R_s |H_s|^2 dx}{\int_0^{d/2} \frac{1}{2} \mu_0 |H_s|^2 dx} = \frac{\sqrt{\omega\Gamma/2}}{\omega_p \sqrt{\mu_0 \varepsilon_\infty}} \frac{1}{d} \quad (20)$$

in the surface loss regime.

The slanted dashed asymptotes in Fig. 3 indicate Eq. (20) for the two frequencies in the  $\omega \ll \Gamma$  regime. The good agreement between the  $\gamma$ - $d$  curves and the asymptotes confirms the applicability of surface resistance to explaining the modal loss behavior in the surface loss regime. We note, however, that surface resistance fails to explain the modal loss behavior in the maximum and plateaued loss regimes, because it is an overly simplified model that cannot fully capture the correct physics occurring at deep-subwavelength scale.

The detailed analysis given so far was for a simple system of the metallic slot waveguide, but the overall trend that the modal loss rate plateaus before reaching  $\Gamma/2$  as the mode shrinks should exist in more general systems as well. For example, consider a system with two metallic objects, such as two metallic spheres, brought in close proximity with a deep-subwavelength dielectric gap in between. In this system, the mode is mostly concentrated in the gap region, like it is in the metallic slot waveguide. Hence, to account for the loss rate of the mode, one may approximate the system by a metallic slot waveguide with varying slot width. Then, at sufficiently low frequencies where the plateau in Fig. 3 becomes wide enough to include the range of the varying slot width of the approximating waveguide, a plateau should appear. Therefore, we can expect a plateaued loss regime to appear for the deep-subwavelength modes between any two metallic objects at sufficiently low frequencies.

In conclusion, we have presented a unified theoretical description that accounts for the significantly different modal loss rates at optical and microwave frequencies in metallic structures. Our main analysis was carried out for simple metallic slot waveguides, but we expect the conclusion to hold for more complex structures as well.

This work was supported by the AFOSR MURI program (Grant No. FA9550-12-1-0471).

<sup>1</sup>D. M. Pozar, *Microwave Engineering*, 3rd ed. (John Wiley & Sons, Hoboken, NJ, 2005).

<sup>2</sup>C. A. Balanis, *Antenna Theory: Analysis and Design*, 3rd ed. (John Wiley & Sons, Hoboken, NJ, 2005).

<sup>3</sup>D. K. Gramotnev and S. I. Bozhevolnyi, *Nat. Photonics* **4**, 83 (2010).

<sup>4</sup>V. M. Shalaev, *Nat. Photonics* **1**, 41 (2007).

<sup>5</sup>A. Raman, W. Shin, and S. Fan, *Phys. Rev. Lett.* **110**, 183901 (2013).

<sup>6</sup>J. B. Khurgin and G. Sun, *Appl. Phys. Lett.* **99**, 211106 (2011).

<sup>7</sup>J. B. Khurgin and A. Boltasseva, *MRS Bull.* **37**, 768 (2012).

<sup>8</sup>F. Wang and Y. R. Shen, *Phys. Rev. Lett.* **97**, 206806 (2006).

<sup>9</sup>J. B. Khurgin, *Faraday Discuss.* **178**, 109 (2015).

<sup>10</sup>M. Ordal, R. Bell, J. Alexander, L. Long, and M. Querry, *Appl. Opt.* **24**, 4493 (1985).

<sup>11</sup>J. A. Dionne, L. A. Sweatlock, H. A. Atwater, and A. Polman, *Phys. Rev. B* **73**, 035407 (2006).

<sup>12</sup>R. Zia, M. D. Selker, P. B. Catrysse, and M. L. Brongersma, *J. Opt. Soc. Am. A* **21**, 2442 (2004).

<sup>13</sup>G. Veronis and S. Fan, *J. Lightwave Technol.* **25**, 2511 (2007).

<sup>14</sup>W. Cai, W. Shin, S. Fan, and M. L. Brongersma, *Adv. Mater.* **22**, 5120 (2010).

<sup>15</sup>E. Feigenbaum and H. A. Atwater, *Phys. Rev. Lett.* **104**, 147402 (2010).

<sup>16</sup>D.-S. Ly-Gagnon, K. C. Balram, J. S. White, P. Wahl, M. L. Brongersma, and D. A. B. Miller, *Nanophotonics* **1**, 9 (2012).

<sup>17</sup>P. B. Catrysse and S. Fan, *Appl. Phys. Lett.* **94**, 231111 (2009).

<sup>18</sup>A. Poddubny, I. Iorsh, P. Belov, and Y. Kivshar, *Nat. Photonics* **7**, 948 (2013).

<sup>19</sup>A. Archambault, T. Teperik, F. Marquier, and J. Greffet, *Phys. Rev. B* **79**, 195414 (2009).

<sup>20</sup>Ş. E. Kocabaş, G. Veronis, D. Miller, and S. Fan, *Phys. Rev. B* **79**, 035120 (2009).

<sup>21</sup>A. R. Davoyan, W. Liu, A. E. Miroshnichenko, I. V. Shadrivov, Y. S. Kivshar, and S. I. Bozhevolnyi, *Photonics Nanostruct. - Fundam. Appl.* **9**, 207 (2011).

<sup>22</sup>E. N. Economou, *Phys. Rev.* **182**, 539 (1969).

<sup>23</sup>J. B. Khurgin, *Opt. Express* **23**, 4186 (2015).